

SHOCKS IN SPHERICALLY ACCRETING BLACK HOLES: A MODEL FOR CLASSICAL QUASARS

P. MÉSZÁROS¹

Harvard-Smithsonian Center for Astrophysics

AND

J. P. OSTRIKER

Princeton University Observatory

Received 1983 March 18; accepted 1983 June 15

ABSTRACT

Spherically symmetric accretion onto black holes is thought to be very inefficient if the flow is nondissipative because of the inadequacy of compression heating and the short time available to radiate. We show here that standing shock solutions exist where the downstream protons are heated to temperatures at which the fluid becomes almost collisionless. The material then moves inwards at the much slower diffusion rate given by the p - e energy exchange time scale. For a given accretion rate, a self-consistent shock radius is found by matching the flow equations above and below that value, showing that such shocks can be self-sustaining. Efficiencies reaching up to 0.1–0.3 can be achieved, with most of the luminosity in the hard X-ray and γ -ray, as well as optical–IR ranges. This provides a new model for the classical (radio-quiet) quasars and active galactic nuclei and possibly for galactic sources such as Cyg X-1.

Subject headings: black holes — galaxies: nuclei — quasars

I. INTRODUCTION

Black hole models of active galactic nuclei may not have accretion disks (see Rees 1977), as when the accreting gas is injected near enough to the hole so that the intrinsic angular momentum is less than that in a Keplerian orbit near the Schwarzschild radius. The accretion flow is then quasi-spherical, and for dissipationless free-fall, it is well known that the radiation efficiency of subcritical accretion would typically be less than 10^{-4} (Shvartsman 1971; Shapiro 1973). More realistic flows may involve entropy generation, if the flow is nonlaminar, which could raise the efficiency up to about 10^{-1} (Mészáros 1975). These calculations, dependent on magnetic fields, turbulence, etc., are quite uncertain. They also suffer from not having any distinguishing length scale, which would enable them to predict specific variability time scales. Such preferred length scales have been introduced by Ostriker *et al.* (1976) (see also Cowie *et al.* 1978; Grindlay 1978), who pointed out the importance of inverse Compton heating for limiting the region of *stable* free-fall inflow. The length scales introduced by this effect are appropriate for the long-term variability of extragalactic sources, but there remains the problem of the short time scales, which require length scales not much larger than the Schwarzschild radius. In this *Letter*

we show that shocks can exist near the horizon, which provide short time variability and also a high efficiency of energy conversion.

The possibility of a standing shock arising in a flow around a black hole has been in the past considered unlikely, because of the absence of a solid surface exerting a back pressure which would uphold the shock. This view, however, is based on an overly hasty extrapolation of the usual experience with one-temperature fluids. A nonfluid, two-temperature description may be more appropriate (e.g., Begelman 1977; Rees *et al.* 1982), and we show below that a self-consistent shock solution can then be found. We also know, in a sense, that accretion can proceed smoothly after a shock transition, since successful subsonic flow solutions have been constructed (cf. Flammang 1982) for accretion onto black holes embedded within normal stars (with boundary condition $r = c$ at the horizon). In the above work and in the related paper by Thorne and Żytkow (1977), it was assumed that the plasma could be treated as an ordinary hydrodynamic fluid incorporating radiation pressure. Here we take the opposite physical model and show that, in this case also, there exist well-behaved subsonic solutions.

The situation we envisage is that of a spherical flow, which in the outer parts is in free fall, the proton random energy being small compared with its radial bulk energy motion. Such cold, supersonic infall is highly unlikely to remain laminar, since small disturbances in

¹Visiting Scientist, Smithsonian Astrophysical Observatory, supported partly by NASA grant NAGW-246; on leave from Max-Planck-Institut für Physik und Astrophysik MPA, Garching.

the density at the accretion radius grow large by the time they reach the horizon (Peterson *et al.* 1980), and this could lead to a shock. Such a shock converts the radial motion energy of the upstream protons into random energy, below the shock. However, once the proton random energy (or “temperature”) is of the order of the gravitational temperature $T_{\text{gr}} \sim GM_p k^{-1} r^{-1}$, one can verify that the protons will be essentially collisionless, since the Coulomb time $t_{pp} \gg t_{\text{ff}}$, the free-fall time. This holds also for t_{pe} , the proton-electron energy exchange time by Coulomb encounters. Furthermore, the protons below the shock will now have large orbital eccentricities and, as in the stellar dynamical case around a black hole, will only be able to accrete into the hole on a diffusion (Coulomb) time scale $\gg t_{\text{ff}}$ (cf. Bahcall and Wolff 1977), since this is the time in which they are able to dissipate their excess orbital angular momentum. (For a different view of a shock model, see Protheroe and Kazanas 1983.) To maintain a steady state, this requires a larger density in the postshock (diffusion) region than in the upstream free-fall region. It is easy to see that, once established, such a situation can perfectly well persist also in steady state.

II. ACCRETION PICTURE

A schematic diagram of the flow is shown in Figure 1. We assume that the upstream material below the accretion radius r_a is in free fall. The temperature of the gas in the region above the shock is determined by the balance of Compton heat gains (due to illumination by hard X-ray photons of average energy $\langle h\nu_\gamma \rangle$ coming from below the shock) and bremsstrahlung cooling. Upstream of the shock, we have $n_p(\bar{r}) = 5 \times 10^{10} m_8^{-1} \dot{m} \bar{r}^{-3/2} \text{ cm}^{-3}$ and $T_e(r) \approx T_1 (\bar{r}/\bar{r}_s)^{-1} \text{ K}$, where $T_1 = (1/4k)\langle h\nu_\gamma \rangle$; \bar{r} is in Schwarzschild units of $2GM/c^2$, $m_8 = M_{\text{BH}}/10^8 M_\odot$, and $\dot{m} = \dot{M}/\dot{M}_{\text{crit}} = \dot{M}c^2/(2L_E)$, with $L_E = 4\pi GM_p c/\sigma_T = 1.3 \times 10^{46} m_8 \text{ ergs s}^{-1}$.

A collisionless shock, arising randomly in the flow, would rapidly acquire spherical symmetry, as a result of the high effective sound speed downstream. The structure of such shocks without large-scale quasi-perpendicular magnetic fields has been explored at low Mach numbers, but at high Mach numbers the situation remains fairly complex (cf. Max *et al.* 1982). The order of magnitude of the shock thickness is expected to be approximately $l_s \sim V_p (m_p/4\pi e^2 n_p)^{1/2} \sim 2 \times 10^1 m_8^{1/2} \dot{m}^{-1/2} \bar{r}_s^{1/4} \text{ cm}$, where \bar{r}_s is the shock standoff distance in Schwarzschild units. The turbulent electric and magnetic fields created in the shock are of magnitude

$$E \sim (c/v_e) B \sim \frac{\delta\phi}{l_s} \sim 3 \times 10^4 m_8^{-1/2} \dot{m}^{1/2} \bar{r}_s^{-5/4} \text{ gauss} \quad (1)$$

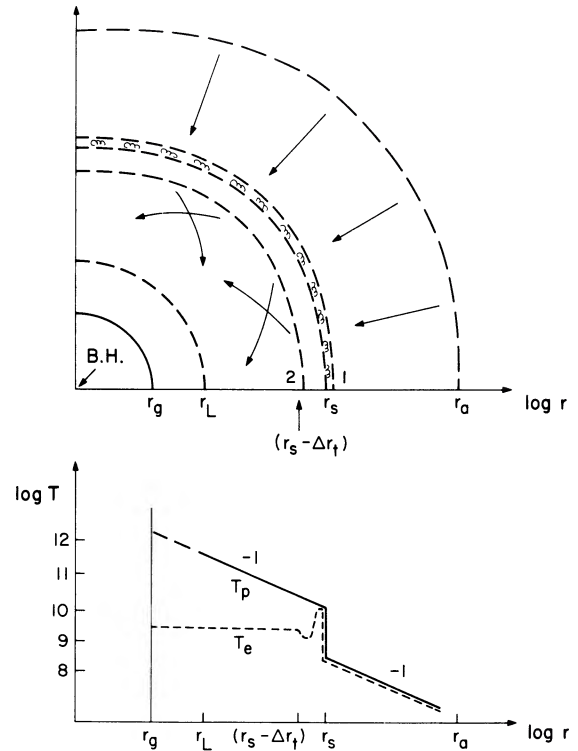


FIG. 1.—(upper) Schematic view (not to scale) of the spherical accretion geometry. Indicated are the accretion radius r_a , shock radius r_s , relaxation layer Δr_s , the lower radius at which the diffusion treatment is valid r_L , and the Schwarzschild radius r_g . The collisionless shock is in the thin, marked region above r_s . The jump conditions are applied between 1 and 2, on either side of Δr_s . Between r_a and r_s , the matter is in free fall, while between $r_s - \Delta r_s$ and r_L , the protons and electrons behave as individual particles, much as a star cluster would, slowly diffusing inwards on the p - e Coulomb scattering time scale. (lower) The proton temperature T_p and electron temperature T_e corresponding to the radial coordinate of Fig. 1 (upper).

(cf. Zel'dovich and Raizer 1967). These turbulent fields will survive downstream for only a short time, an absolute upper limit on which is given by the magnetic decay time $t_B \sim 4\pi\sigma_c l_s^2/c^2$, where σ_c is the conductivity; a conservative estimate is $t_B \lesssim 10^2 \omega_{\text{op}}^{-1} \sim 10^{-7} m_8^{1/2} \dot{m}^{-1/4} \bar{r}_s^{-1/4}$. The turbulent fields will therefore be dissipated very shortly behind the shock transition layer. What about any possible large-scale magnetic fields that are present in the upstream flow? These would have to be significantly below equipartition for the upstream region to be subsonic and freely falling. As long as $B_1 < [(\gamma - 1)/(\gamma + 1)] B_{\text{eq}} \sim (1/4) B_{\text{eq}}$, these large-scale fields will be below equipartition also after adiabatic compression in the shock transition. However, the chaotic E and B fields produced in the shock itself are by definition at equipartition, since $B \sim E \sim kT/el_s$ implies $B^2/8\pi \sim (1/2)\rho V_p^2$. The large-scale fields will be dominated by the chaotic ones, which vary over the

extremely small length scale l_s (eq. [3]), and the chaotic currents will cause wiggles of scale l_s to appear in the large-scale field loops. Having acquired this small-scale structure, they are dissipated on the same short time scale t_b as the chaotic fields, provided magnetic reconnection occurs on this scale. If it does not, the large-scale radial field component persists. Thus, as long as the upstream magnetic energy is significantly sub-equipartition and magnetic reconnection occurs in the chaotic layer below the shock, and as long as one may neglect any possible anomalous scattering mechanisms, our approximation of a nonfluid, stellar dynamic type of regime in the downstream region is justified.

In the transition layer Δr_t , the electrons cool quickly and thus half of the dissipated turbulent field energy is transformed into photons via the synchrotron and inverse Compton mechanisms. An equilibrium is reached with $T_e \ll T_p$ behind the turbulent field zone. The electrons are heated by Coulomb encounters with protons at $T_p \sim T_{gr}$ and cooled by bremsstrahlung and inverse Compton. For $\tilde{r}_s \lesssim 4 \times 10^2$, they reach an equilibrium temperature at $\theta_e = (kT_e/m_e c^2) \lesssim 1$, above which the losses increase rapidly due to relativistic processes. Downstream of Δr_t , we have $T_p(\tilde{r}) \sim T_{gr} \sim 2 \times 10^{12} \tilde{r}^{-1}$ K and $T_e(\tilde{r}) \sim \theta_e (m_e c^2/k) = \theta_e 6 \times 10^9$ K. The relaxation shell is of relative width $\Delta r_t/r_s \sim T_e/T_p \sim 2.7 \times 10^{-3} \theta_e \tilde{r} \ll 1$.

Below the relaxation region, we have a quasi-collisionless flow, where matter flows inwards on a diffusion time scale. For the solutions found here, the proton-electron Coulomb time $t_{pe} \ll t_{pp}$, the proton-proton time, so we neglect proton heat conduction effects. Both the diffusion of matter inwards and the energy exchange occur therefore on the time scale $t_{pe} \approx (m_p c^2 \theta_e)/n_e \sigma_T m_e c^3 \ln \Lambda \approx 1.5 \times 10^{-8} \theta_e \rho^{-1}$, valid for relativistic electrons if $T_e \ll T_p$ (Gould 1981).

We apply jump conditions to the flow on both sides of the relaxation region (see Fig. 1). In the downstream (2) side, we assume that the matter moves inwards with a diffusion velocity $u_2 = \delta r t_{pe}^{-1}$, where $\delta \sim 1$ is a constant. This means that for $r < r_2 = r_s - \Delta r_t$, one has $\rho \propto r^{-3/2}$, where the exponent is fortuitously the same as in free fall, although the constant in front is different. The downstream one-dimensional velocity dispersion V_2 is linked to the "pressure" via $p_2 = \rho_2 V_2^2$ and to the "temperature" via $T_2 = k^{-1} m_p V_2^2$. This is taken to be the gravitational value corresponding to a $\rho \propto r^{-3/2}$ law, $(V_2/c)^2 = (2/5)GM/rc^2 = (1/5)\tilde{r}^{-1}$. Upstream, we may take $u_1 = (2GM/r)^{1/2}$, and $p_1 = T_1 \equiv 0$ is taken for simplicity. The density jump is, therefore,

$$\frac{\rho_2}{\rho_1} = \frac{u_1}{u_2} = 1.67 \times 10^1 \dot{m}^{-1/2} \delta^{-1/2} \theta_2^{1/2} \eta_2^{-1/2}, \quad (2)$$

where η_2 is the ratio of electrons (and positrons, if any) to protons. We do not expect a large pair density, i.e.,

$\eta_2 \sim 1$ (see below). The density jump is higher than for an adiabatic (fluid) shock, since u_2 is not a hydrodynamic velocity but a diffusion velocity and because the relaxation zone is not adiabatic. Momentum conservation can be written as

$$\rho_2 u_2^2 + \rho_2 V_2^2 - \frac{4}{3} \gamma \frac{r^2 \rho_2}{2 t_{pe}} \frac{u_1}{\Delta r} = \rho_1 u_1^2. \quad (3)$$

The third term on the left is the viscous stress tensor $\sigma \approx (4/3)(\lambda^2 \rho/t)(du/dr)$; for the mean free path λ , we take $\lambda^2 \approx \gamma r^2$, with $\gamma = \text{const} \sim (1/2)$; for the viscous (forward momentum) exchange time, we take $2t_{pe}$, this being the appropriate value for protons on electrons (e.g., Spitzer 1962); and for du/dr , we replace $\sim u_1/\Delta r$, since $u_2 \ll u_1$. We take $\Delta r \sim \Delta r_t$. Condition (3) implies that the shock standoff distance is

$$\tilde{r}_s \approx 50 \dot{m}^{1/2} \theta_2^{-3/2} \eta_2^{1/2} \gamma \delta^{-1/2}. \quad (4)$$

As \dot{m} decreases from unity, the shock radius approaches the Schwarzschild radius $\tilde{r} = 1$, reaching it for $\dot{m}_s = 4 \times 10^{-4} \theta_2^{1/3} \eta_2^{-1} \gamma^{-2} \delta$. Since at \tilde{r}_s we satisfy $t_{pe} \ll t_{pp}$, we do not normally expect a region dominated by proton conduction to exist.

The electron temperature in the inner region is almost uniform because the electron exchange time is very short compared with the $e-p$ time. Behind the shock, photons are produced by $e-p$ and $e-e$ bremsstrahlung. Comptonization plays a role in limiting the temperature below about $\theta_e \lesssim 1$. The temperature adjusts itself to a value where the Comptonization is in the unsaturated regime. Pair production will also tend to stabilize the temperature at $\theta_e \lesssim 1$, although mostly $n_{\pm} < n_p$, $\eta \sim 1$. The proton density downstream of the shock is given by $n_p(\tilde{r}) = 8.3 \times 10^{11} \dot{m}^{1/2} m_8^{-1} \theta_2^{1/2} \eta^{-1/2} \delta^{-1/2} \tilde{r}^{-3/2} \text{ cm}^3$, which is a factor of approximately $17 \dot{m}^{-1/2}$ times the upstream free-fall density. This is also the ratio of $p-e$ scattering time to free-fall time. Below $\tilde{r} \lesssim 3.5$, the protons, at the temperature given by equation (4), have enough energy to make pions via $p-p$ collisions. Using the rates of Kolykhalov and Sunyaev (1979), we have $t_{\pi}/t_{ff} \approx 10^2 \dot{m}^{-1} \tilde{r}^{0.86}$. Thus for $\tilde{r} < \tilde{r}_1 \sim 3$, this is the principal energy loss mechanism. The dynamics is further complicated by the presence of general relativistic and loss cone effects, both of which become important below $\tilde{r}_1 \approx 3$. These tend to accelerate the flow in this region, so that the lower boundary provides no new constraints on the inflow rate.

III. IMPLICATIONS

The fact that the protons diffuse inward by transferring their energy to the electrons, which then radiate it away, implies a very high efficiency, of order near unity. It does not reach unity since the simple diffusion

breaks down as one approaches the horizon because of new effects that start playing a role near the horizon. These, however, should still leave the efficiency above 0.1–0.3.

The X-ray spectrum produced by the upstream gas is a superposition of optically thin bremsstrahlung spectra with varying $\rho(r)$ and $T(r)$, giving a power-law $F_\nu \sim \nu^{-b}$, with $b \sim 0.6$ – 0.7 (cf. Mészáros 1983). At 2 keV (4.83×10^{17} Hz), the spectral flux density is $l_x \sim 10^{27} m_8 \dot{m}^{7/4} (\tilde{r}_i/3)^{-1}$ ergs s $^{-1}$ Hz $^{-1}$, where \tilde{r}_i is the lowest radius entering equation (5). The corresponding luminosity is a fraction τ (upstream) of the value given by equation (5).

There will be another spectral component in the IR–optical range, resulting from Comptonized synchrotron photons produced in the turbulent fields near the collisionless shock itself. The synchrotron peak, in the chaotic fields of the strength given by equation (1), depends on the electron Lorentz factor Γ , $v_m \sim 1.5 \sin \alpha [(eB)/(2\pi m_e c)] \Gamma^2 \geq 10^{12} m_8^{-1/2} \dot{m}^{9/8}$, where we took the adiabatic shock temperature, $\Gamma_{th} \sim 10^3 \tilde{r}^{-1}$. Additionally, a fraction of the electrons may acquire a superthermal power-law distribution (Blandford and Ostriker 1978; Eichler 1979) so that $\Gamma_{st} \geq \Gamma_{th}$, and the spectrum will be a power law extending blueward of the peak ν_m . A blueward power law is also expected because half of the synchrotron photons, initially emitted downwards, encounter the hot ($\theta_e \leq 1$, $\tau_s \geq 1$, see below) downstream diffusion region, which leads to a spectrum $F_\nu \propto \nu^{-\alpha}$ (Shapiro *et al.* 1976; see also Katz 1976), with $\alpha \geq 1$, typical of observed optical spectra. The total IR–optical luminosity due to the shock is $L_s \approx GMM/(2r_s)^{-1} \sim 1.5 \times 10^{44} m_8 \dot{m}^{1/2} \theta_2^{3/2}$ ergs s $^{-1}$. We estimate for the optical flux density at 3000 Å (10^{15} Hz) $l_o \approx 10^{30} (a_0/5) \dot{m}^{1/2} \theta_2^{3/2}$ ergs s $^{-1}$ Hz $^{-1}$, where a_0 is the amplification factor from ν_m to 10^{15} , which itself also depends on \dot{m} in a complicated manner through $\tau_s(\dot{m})$ and $\theta(\dot{m})$.

The downstream diffusion region will emit mainly in the poorly observed, hard X-ray region, ≥ 200 keV. The typical scattering opacity seen by a photon is approximately a few. The spectrum will be isothermal bremsstrahlung, moderately Comptonized, i.e., with a moderate hump at $\langle h\nu_\gamma \rangle \sim (1-3)kT_e \sim 0.5$ – 1.5 MeV and fewer photons below. The luminosity in this component is close to the total one,

$$L_i \sim L_d \approx \frac{GMM}{r_i} \approx 4 \times 10^{45} m_8 \dot{m} (\tilde{r}_i/3)^{-1} \text{ ergs s}^{-1}, \quad (5)$$

where $\tilde{r}_i \geq 3$ is the lowest radius to which our classical p - e diffusion treatment can be extended. The pair recombination luminosity in the region $\tilde{r}_i < \tilde{r} < \tilde{r}_s - \Delta\tilde{r}_i$ will be significant, contributing to the hump above approximately 0.5 MeV. For $\tilde{r} \leq 3$, general relativistic effects and pion production by p - p collisions are im-

portant, and there may be loss cone effects as well.

The total emission in the form of γ -rays depends on the dynamic inflow time in the region $\tilde{r} \leq 3.5$, where the main energy loss mechanism is pion production by p - p collisions. A dynamic time t_π would lead to a luminosity $L_\gamma \sim 10^{37} m \dot{m} (t_{ff}/10^2 t_{dy}) \sim 10^{45} m_8 \dot{m} (t_{ff}/10^2 t_{dy})$, where we took the upper limit given by $t_{dy} \sim t_\pi$ and included gravitational trapping of photons. The actual γ -ray luminosity may be lower, due to general relativistic effects on the particle orbits, which would drive t_{dy} toward t_{ff} , which could also lead to increasing photon trapping by convection. The neutrino luminosity will be of the same order. The intrinsic γ -ray photon spectrum due to this process would peak at about 20 MeV, with about 10% of the photons at $E_\gamma \geq 100$ MeV. The actual spectrum that escapes, however, may not extend beyond $E_\gamma \leq$ MeV, due to photon-photon absorption with the X-ray photons, at the higher \dot{m} values. This opacity decreases with \dot{m} , $\tau_{\gamma\gamma} \sim 1.3 \times 10^4 \dot{m} (\epsilon/0.1)^{-1} (\tilde{r}/\tilde{r}_i)^{-1}$, so that for $\dot{m} \leq 10^{-1}$ one may see the full γ -ray spectrum extending to more than 10^2 MeV. For $\dot{m} \geq 10^{-1}$, the degradation of the high-energy γ -ray photons will add to the approximately MeV hump.

The short-term variability of the optical emission will be, for large-amplitude variations ($\Delta L/L \sim 1$), $t_o \sim t_{ff}(\tilde{r}_s) = 4 m_8 \dot{m}^{3/4} \theta_2^{-9/4}$ days. For $m \sim 10$, corresponding to stellar black holes, this time is about 30 milliseconds. In terms of the optical luminosity, one has $t_o \propto l_o^{1.5}$, and for \dot{m} approaching unity, one expects large-amplitude relaxation oscillations to set in. The X-ray emission can have short-period, $\Delta L/L \sim 1$ variations on the time scale $t_x \sim t_{pe}(\tilde{r}_s) = 4 \times 10^4 m_8 \dot{m}^{1/4} \theta_2^{-3/2}$ days, or $t_x \propto l_x^{1/7}$. The small-amplitude variations can occur on the light-travel time $t'_x \sim t_L(r_s) \sim 1.4 \times 10^4 m_8 \dot{m}^{1/2}$ hr, with $t'_x \propto l_x^{2/7}$. The hard X-rays will vary on $t_{HX} \sim t_{pe}(\tilde{r}_s) = 40 m_8 \dot{m}^{1/4}$ days, or $t_{HX} \propto L_{HX}^{4/3}$. The very high energy (> 100 MeV) γ -rays, when \dot{m} is low enough for their escape, should have large-amplitude variations on a time scale of t_{dyn} at $\tilde{r} \sim 3$, which lies between $t_\gamma \sim t_{ff}(3) \sim 1.5 m_8$ hr and $t'_\gamma \sim t_{pe}(3) \sim 2 \times 10^4 m_8 \dot{m}^{-1/2} \theta_2^{1/2}$ hr, $t'_\gamma \propto L_\gamma^{-1/2}$. For $\dot{m} \geq 10^{-1}$, when the γ -ray spectrum cuts off at about 1 MeV due to photon-photon absorption on the X-rays, the variability is the same as that of the hard X-rays.

Our model as presented here applies mainly to radio-quiet QSOs, Seyfert 1 galaxies, and X-ray selected active galactic nuclei. Scaled-down versions ($m \sim 10$) would apply to galactic black hole sources such as Cyg X-1, Cir X-1, and LMC X-3. Notice that, for $m \sim 10$, the ν_m of the shock luminosity is in the UV. It is worth noting that, since Seyfert galaxies and quasars contribute significantly to the diffuse X-ray and γ -ray background, the γ -ray feature at $E \sim 20$ MeV seen in our models may account for the well-known feature in the γ -ray background at 4–6 MeV (e.g., Fabian 1980). A test of our

spherical models may be possible through the time variabilities that we predict as a function of luminosity. A specific prediction is that, in the γ -ray domain, we expect a broad peak around 0.5–1.5 MeV, due to the hot downstream electrons, and another broad peak around 20 MeV, from p - p reactions near the horizon.

This research has been supported partly by NASA grant NAGW-246 (P. M.) and NSF grant AST 80-22785 (J. P. O.). We are grateful to R. Kulsrud, J. Krolik, D. Q. Lamb, A. P. Lightman, R. Lovelace, and C. Max for comments.

REFERENCES

- Bahcall, J. N., and Wolff, R. A. 1977, *Ap. J.*, **214**, 90.
 Begelman, M. C. 1977, *M. N. R. A. S.*, **181**, 347.
 Blandford, R. D., and Ostriker, J. P. 1978, *Ap. J. (Letters)*, **221**, L29.
 Cowie, L. L., *et al.* 1978, *Ap. J.*, **226**, 1041.
 Eichler, D. 1979, *Ap. J.*, **229**, 419.
 Fabian, A. C. 1980, *Ann. NY Acad. Sci.*, **375**, 235.
 Flammang, R. A. 1982, *M. N. R. A. S.*, **199**, 833.
 Gould, R. J. 1981, *Phys. Fluids*, **24**, 102.
 Grindlay, J. E. 1978, *Ap. J.*, **221**, 234.
 Katz, J. I. 1976, *Ap. J.*, **206**, 910.
 Kolykhalov, P. I., and Sunyaev, R. A. 1979, *Soviet Astr.—AJ*, **23**, 189.
 Max, C., *et al.* 1982, *Bull. AAS*, **14**, 937.
 Mészáros, P. 1975, *Astr. Ap.*, **49**, 59.
 Mészáros, P. 1983, *Ap. J. (Letters)*, in press.
 Ostriker, J. P., *et al.* 1976, *Ap. J. (Letters)*, **208**, L61.
 Petterson, J., *et al.* 1980, *M. N. R. A. S.*, **191**, 571.
 Protheroe, R. J., and Kazanas, D. 1983, *Ap. J.*, **265**, 620.
 Rees, M. J., *et al.* 1982, *Nature*, **295**, 17.
 Shapiro, S. L. 1973, *Ap. J.*, **180**, 531.
 Shapiro, S. L., *et al.* 1976, *Ap. J.*, **204**, 187.
 Shvartsman, V. F. 1971, *Soviet Astr.—AJ*, **15**, 377.
 Spitzer, L., Jr. 1962, *Physics of Fully Ionized Gases* (New York: Wiley Interscience).
 Thorne, K. S., and Żytkow, A. N. 1977, *Ap. J.*, **212**, 832.
 Zel'dovich, Ya. B., and Raizer, Yu. P. 1967, *Physics of Shock Waves and High-Temperature Hydrodynamic Phenomena* (New York: Academic).

P. MÉSZÁROS: Pennsylvania State University, Astronomy Department, University Park, PA 16802

J. P. OSTRIKER: Princeton University Observatory, Peyton Hall, Princeton, NJ 08540